DIFFERENTIAL SENSING IN HOST:GUEST ARRAYS WITH NOVEL DYES

By

Alexie Andrea Pardillo Raz

A capstone project submitted for Graduation with University Honors

May 12, 2023

University Honors
University of California, Riverside

APPROVED

Dr. Richard J. Hooley
Department of Chemistry

Dr. Richard Cardullo, Howard H Hays Jr. Chair
University Honors

ABSTRACT

Synthesized dyes and hosts, in this case water-soluble cavitands, come together to form an array-based sensor system. The cavitands bind to a series of guest fluorophores, molecules that absorb and emit light, in this case the synthesized dyes. Upon binding, the dye can be competitively displaced by a molecule of interest and data is collected by measuring the emission differences upon displacement, which can vary depending on the type of host and guest used. While some host:dye complexes experience an enhanced emission, others instead result in a loss of fluorescence. A multitude of novel dyes were synthesized in the laboratory and their differential fluorescent responses were studied. This differential sensing tool can be used to distinguish slight structure variations in biorelevant targets that might be undetectable using other methods of spectroscopy. Understanding the different mechanisms of how these dyes work in tandem with the cavitands to discriminate between targets based on their structure can prove useful in a wide range of biosensing applications.

ACKNOWLEDGMENTS

I would like to express my gratitude to the many individuals who have played a crucial role in the execution of this research. Firstly, I want to thank my faculty mentor, Dr. Richard Hooley, for his exceptional guidance and mentorship throughout my time in the laboratory. Secondly, I am deeply appreciative of my graduate student mentor, Briana L. Hickey, who not only allowed me to contribute to her work but also provided me with unwavering support throughout the entire process. I also want to extend my thanks to all the individuals in the lab group, as well as my family and friends, who have supported me during a challenging period in my life. Finally, I want to express my gratitude to the University Honors program and its staff for providing me with the means and guidance that have supported me as an undergraduate researcher.

TABLE OF CONTENTS

INTRODUCTION

Host:guest sensor arrays have emerged as powerful tools for sensing small structural differences in various biomolecules, enabling their differentiation and classification through pattern recognition using simple fluorescence measurements. Supramolecular probes are well-suited for array-based pattern recognition, due to their ability to selectively bind to specific target molecules or surfaces with high affinity and specificity (Zhong and Hooley 1035). Furthermore, supramolecular probes can be easily modified to tailor their properties to specific applications. This allows for the creation of custom-designed probe arrays that can be optimized for particular sensing tasks. Arrayed host:guest fluorescence sensor systems have already been established in previous papers, and the broad applicability ranges from monitoring enzyme reactions, to analyzing peptide and protein modifications (Chen, Hickey, Wang, et al. 488; Gill, Hickey, Zhong, et al. 4352). These sensor arrays are constructed using a suite of host molecules, and multiple dye candidates, that bind both to the hosts and target molecules, and minor changes in the target structure can be selectively detected through pattern recognition-based sensing. Earlier publications have documented the method for synthesizing the dye components used in the sensing array (**Figure 1**). In the presence of increasing host concentration, each dye exhibited a different fluorescence response.

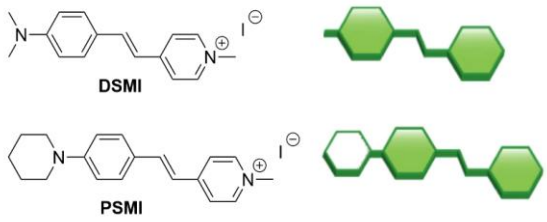

Figure 1. Structures and cartoon illustrations of previously synthesized fluorophores, trans-4-[4-(dimethylamino)styryl]-1-methylpyridinium iodide (**DSMI**) and trans-4-[4-(piperidino)styryl]-1-methylpyridinium iodide (**PSMI**).

Analysis of the different fluorescence responses using these dyes, based on their affinity for both the target molecule and the cavitand hosts, allowed for discrimination between samples

of almost identical structural composition (Hickey, Chen, et al. 13341). The exploitation of multiple recognition mechanisms in a host:guest system is crucial, and the combination of dyes and cavitands must be further studied. While there exist several mechanistic possibilities for the observed changes in emission with variable cavitands and dyes, the principal conclusion is that even minor structural differences can significantly impact the fluorescence output. This project focuses on the synthesis and comprehensive characterization of novel dyes.

DISCUSSION

Novel dyes were created for the investigation of non-traditionally folded DNA structures. X-ray crystallography and multidimensional NMR spectroscopy can provide an exhaustive analysis of structural alterations caused by nucleotide modification. However, these techniques are costly, time-consuming, and necessitate large quantities of material. Thus, there is a need for a rapid and cost-effective optical approach to detect the existence of base modifications in DNA. While circular dichroism (CD) is a typical optical method that can offer some insights, it is insufficient in detecting subtle structural changes.

The sensor components in the array consist of cationic dye molecules that bind to the target analytes, as well as synthetic host molecules, in this work water-soluble deep cavitands, that can bind these dyes competitively while modulating their fluorescence. These cationic, water-soluble dyes vary with slight variations in the headgroup size, resulting in similar fluorescence properties. The size and shape variations impart small differences in affinity between the sensor components, while maintaining similar detection ranges to the target molecules. Complementary to the dyes, a set of water-soluble host molecules, cavitands, can bind to the fluorophores and modulate their emission. Four main cavitand structures, tetracarboxylate benzimidazole (**TCC**), N-methylimidazolium octamide

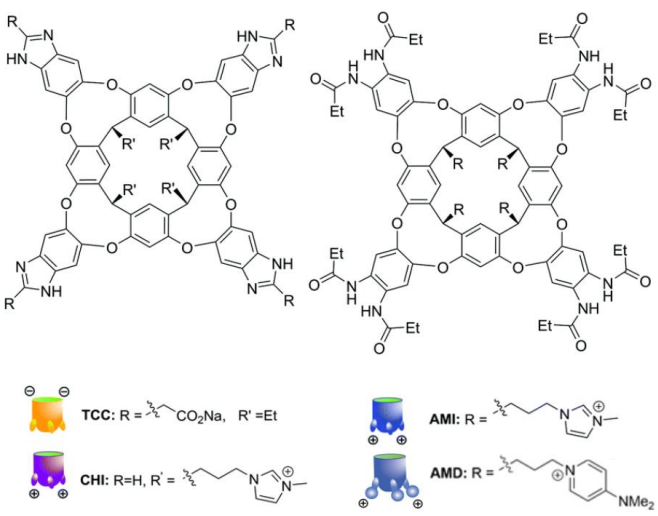

Figure 2. Structures and cartoon illustrations of synthetic hosts **TCC**, **CHI**, **AMI**, and **AMD**, which can bind to the dyes and modulate their fluorescence output.

cavitand (**AMI**), 4-dimethylaminopyridine-octamide cavitand (**AMD**), and N-methylimidazolium benzimidazole cavitand (**CHI**) were synthesized according to literature procedures. The structures are shown in **Figure 2**, alongside cartoons depicting their bowl-like shape (Chen, Hickey, Gao, et al. 2164). The cavitand hosts exhibit affinity for the dyes, allowing competition between the dye and the molecule of interest. In addition to the other recognition equilibria mentioned, a cavitand:dye:DNA heteroternary complex can also be formed (Chen, Gill, Hickey, et al. 12791). These sensor components, of which the procedure for the synthesis was established in previous papers, can be assembled in an array for pattern recognition analysis, enabling rapid and selective detection of small changes in target structure (Gill, Hickey, Wang, et al. 13259).

The aim of this study was to synthesize novel dyes for use in a sensor-based array system, by modifying the ends of the dye molecules to alter their properties and affinity for a host. Typically, the synthesis of these dyes involves two steps, namely the creation of a pyridinium salt, followed by the addition of an aldehyde via a Knoevenagel condensation to form a conjugated alkene in the middle of the two aromatic rings of the structure. By modifying the functional groups of either the salt or the aldehyde, novel dyes can be formed and tested for their sensor-based applications. The study began by establishing an altered methodology for the synthesis of novel dyes with a structure akin to previously synthesized dyes. This approach was then employed to create dyes with more diverse ends. A detailed description of the general scheme used for dye synthesis is provided in the experimental section, along with the structures and corresponding spectral data. Two different aldehydes, namely 4-(dimethylamino)benzaldehyde and 4-(methylthio)benzaldehyde, were employed in the second step. It is worth mentioning that, overall, the synthesized dyes featuring the aldehyde with the methylsulfanyl (SMe) functional group exhibited greater fluorescence and brightness compared to those with the aldehyde containing the

dimethylamino (NMe_2) functional group. The combination of different components in the two steps of the synthetic process resulted in differences in not only the structure, but also the size, and optical properties of the resulting dyes, such as the color of the powdered dye itself. The effects of these variations on fluorescence and binding affinity will be discussed further.

UV-Vis absorbance measurements were recorded to determine the optimal excitation and emission frequencies for the dyes (**Figure 3**). The binding of the dyes to the cavitand hosts is influenced by both competitive displacement from the DNA, and the formation of host:dye:DNA complexes, which results in an alternative sensing mechanism to the dyes alone. Analysis of the results indicates that each cavitand exhibits a slightly different affinity to the dyes within a specific range. This allows for competition with dye:DNA binding, introducing variable outputs that can be used for differential analysis. Therefore, it can be concluded that the combination of cavitands and dyes provides a promising approach for biosensing.

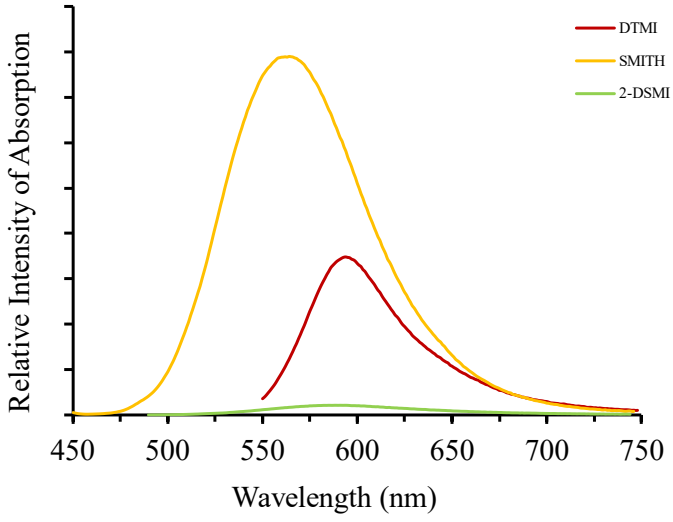

Figure 3. UV-Vis absorbance spectra of dyes **DTMI**, **SMITH**, and **2-DSMI** taken in ultrapure H_2O.

Titration experiments were performed to investigate the interaction method between the dyes and cavitands in the system. Flexible and bowl-shaped, these receptors can be outfitted with different motifs at the upper or lower rim, causing either fluorescence enhancement, or quenching upon binding of the dye. The interaction of these components can result in the downfield shifting

of proton signal, as a function of the cavitand:dye ratio, which can be monitored via ^{1}H NMR. These changes in chemical shift are a likely indication of a binding event occurring. The procedure used for the experiment conducted in an NMR tube is outlined in the experimental section and was followed accordingly. This can be seen in the stacked spectra in **Figure 4**, with focus on dyes (E)-1-methyl-4-(4-(methylthio)styryl)pyridin-1-ium iodide **(SMITE**) and (E)-2-(4-(dimethylamino)-styryl)-1-methylpyridin-1-ium iodide (**2-DSMI**), and the **TCC** cavitand mentioned earlier. Examining the dye titration into the cavitand solution through NMR analysis yields a more comprehensive understanding of the cavitand:dye binding mechanism. In comparison to **2-DSMI**, **SMITE** has a lower affinity and displays rapid in/out exchange on the NMR timescale. The binding affinity of **TCC** for dyes presents a dual nature: on one hand, it allows the host to effectively bind with target molecule, while on the other hand, a strong affinity for the dyes

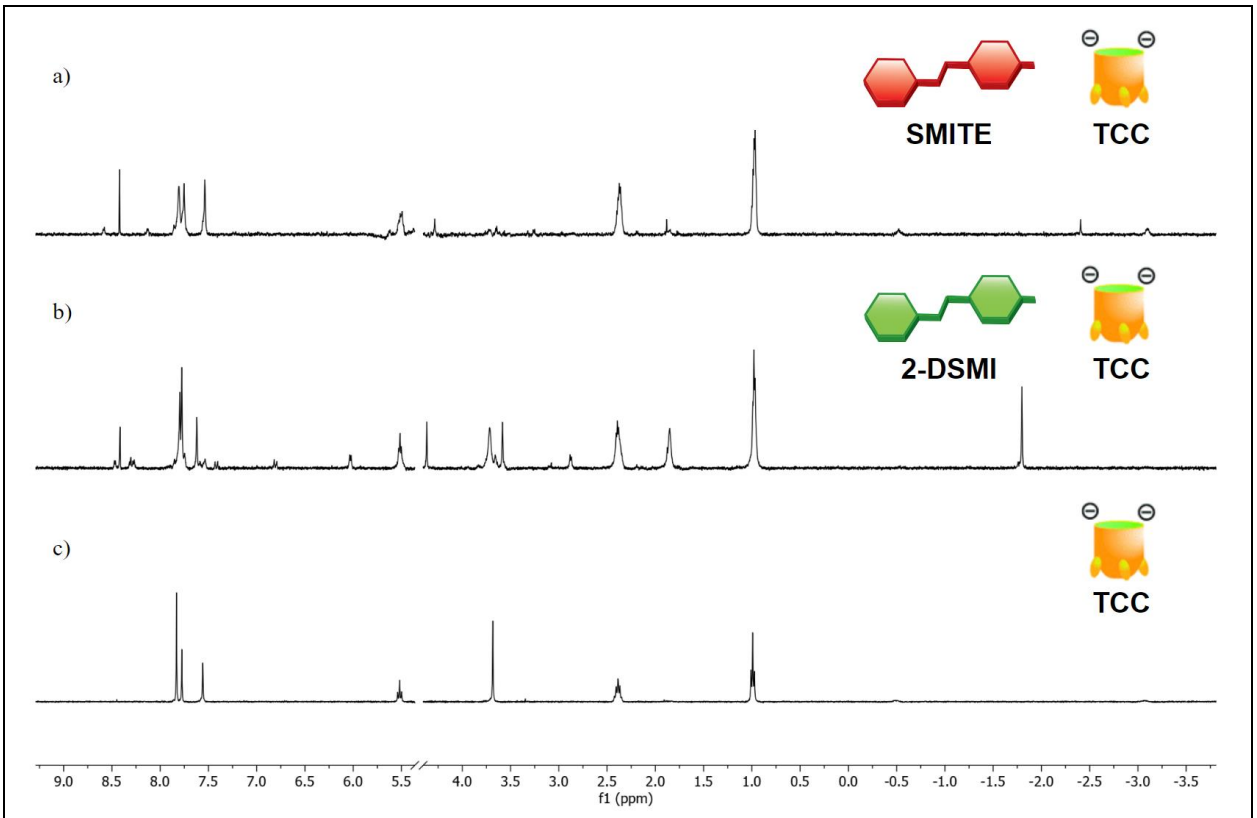

Figure 4. ^{1}H NMR spectra (600 MHz, D_2O, 298K) of cavitand:dye binding. a) 1 eq. of **SMITE** titrated into 1 eq. of **TCC**, b) 1 eq. of **2-DSMI** titrated into 1 eq. of **TCC**, c) **TCC**.

impedes the target molecule's ability to displace **2-DSMI** or **SMITE** from the host in a significant manner. These findings provide an insight into water-soluble hosts and the complexes they form in the presence of dyes as guests, and a better understanding of the sensing modes that can be derived from these components.

As mentioned briefly before, while some cavitand:dye complexes exhibited enhanced emission upon binding, others experienced a loss of fluorescence after an initial increase, referred to as quenching. This could have occurred due to several factors, including collisional quenching between the dye and the host, changes in the local environment surrounding the dye upon binding, or the formation of a micellar aggregate (Liu, Perez, Mettry, Easley, et al. 10746). It is difficult to pinpoint the exact factors responsible, but understanding the mechanism is crucial for designing host:guest sensing arrays with high sensitivity and selectivity. In addition, instead of focusing on a single specific fluorescent probe, non-cavity-based interactions can also tune the dye and target molecule interactions, resulting in numerous recognition equilibria that can modulate the fluorescence response.

Further titration experiments were conducted to explore anion recognition via the use of cationic, flexible cavitands. By binding a dye inside the cavity, it was possible to observe the modulation of fluorescence response due to the presence of anions at the base of the cavitand (Aziz et al. 1). Increasing concentrations of halides were added to a cavitand solution to test this effect. The cavitands used in these experiments were receptors with electron-rich cavities, capable of binding anions at the positively charged lower rim (Liu, Perez, Mettry, Gill, et al. 3960). This recognition mechanism introduces the potential to use the bowl-shaped cavity of the cavitand to bind an indicator molecule, such as a dye, and then utilize lower rim anion binding to produce a change in fluorescence response, thus allowing for optical detection of anions. Such an approach

could be useful in designing an indicator displacement assay for biorelevant targets. The results of these titration experiments may provide insight into the feasibility of utilizing this recognition mechanism for such an assay and may also facilitate the development of novel anion sensors.

A variety of cavitands were investigated, differing in their cationic groups at the lower rim and their conformation in aqueous solution. Among them, the benzimidazole cavitand, **CHI**, was found to be stable in water and retains the "vase" conformation due to intermolecular hydrogen bonding with four intercalated water molecules along its benzimidazole walls. On the other hand, the octamido cavitands **AMI** and **AMD** exist in an open "kite" formation until a suitable guest is added. These cavitands were paired with a group of dyes that proved to be effective in detecting modified DNA with the cationic hosts. Although the hosts and dyes shared a similar structure, the fluorescence changes observed in the presence of anions varied significantly. Upon binding to the host cavities, the cationic dyes led to a reorganization of the flexible amide cavitands, resulting in a variable emission. The fluorescence response of the dyes in the presence of μM – mM concentrations of select halides (NaCl, NaBr, and NaI) was evaluated, and only the iodide anion showed a significant change. NaI caused a decrease while NaBr caused an increase in fluorescence. However, the addition of NaCl did not cause any significant change. Notably, in the absence of anions, none of the dyes exhibited a noticeable loss of fluorescence. As the concentration of iodide increased, the octamide cavitand **AMI** exhibited a substantial reduction in fluorescence. Similar observations were made with the benzimidazole cavitand **CHI**, although the extent of fluorescence reduction was not as significant as with **AMI**. This could be due to the difference in their conformations. Without any guest molecules, **AMI** is in an unfolded "kite" conformation that causes deformation in the cavitand and the lower rim functional groups (Hickey, Raz, et al.). When a dye is present in the cavity, it shifts to a folded "vase" conformation, resulting in less flexibility

for the lower rim groups to bind anions. This leads to a reorganization of the cavitand when iodide binds at the base, which disrupts dye binding and leads to a decrease in emission.

Titrations of host:anion complexes were performed to investigate the halide binding properties and corroborate them with the fluorescence findings. The experimental procedure followed in the NMR tube is consistent with the general method outlined in the experimental section. Solutions of the halide salts were added to a 1 mM solution of **AMI** and revealed strong iodide binding affinity as can be seen in **Figure 5**. Other halide salts were bound with lower affinity, after analyzing the ^{1}H NMR spectra. The process of anion exchange occurred rapidly on the NMR timescale, and after the addition of 5 mM NaI, the peak shifts reached saturation. On the

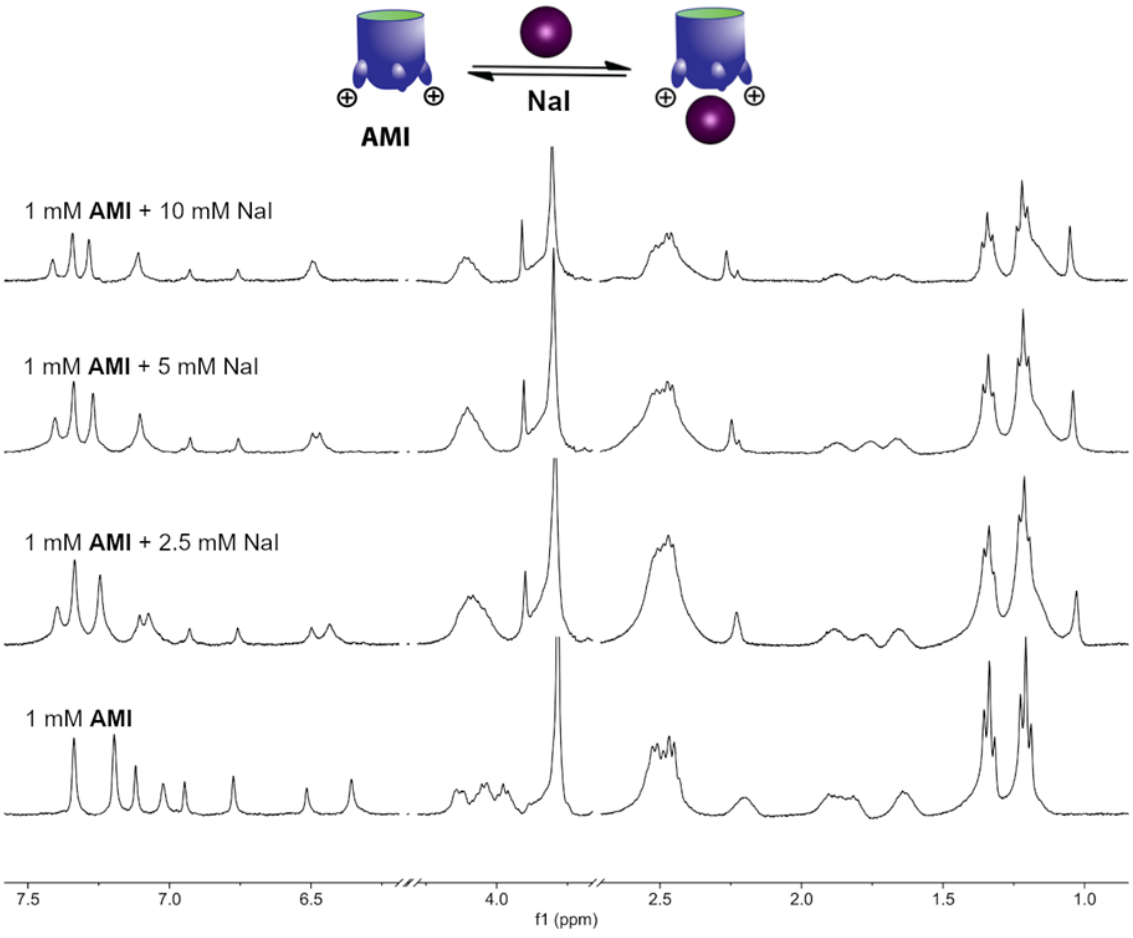

Figure 5. ^{1}H NMR spectra (600 MHz, D_2O, 298K) of **AMI**:NaI binding.

other hand, there was no saturation observed with NaBr, and NaCl did not exhibit any binding. The protons that underwent a shift in their position were situated on the base of the cavitand's lower rim. The host's folding state remained unaffected throughout the process. Another octamide-based cavitand, **AMD**, was tested, which showed a comparable response to AMI with a rapid and strong decrease in fluorescence in the presence of iodide. In **Figure 6**, the titration of NaI with **AMD** is depicted, and indicates the cleavage of the cationic 4-dimethylaminopyridine (DMAP) groups present at the lower rim, through a substitution reaction with NaI. Exposing **AMD** to I^-, and to a lesser extent, Br^-, in an NMR sample in D_2O resulted in the host's precipitation due to the nucleophilic substitution of the cationic DMAP groups by iodide and the formation of an insoluble iodo-cavitand. As a result, only the signals of DMAP were detected in the solution. Overall, the initial fluorescence tests suggest that the cationic hosts exhibit selective sensitivity to the presence of iodide in aqueous solutions of other high salt concentrations.

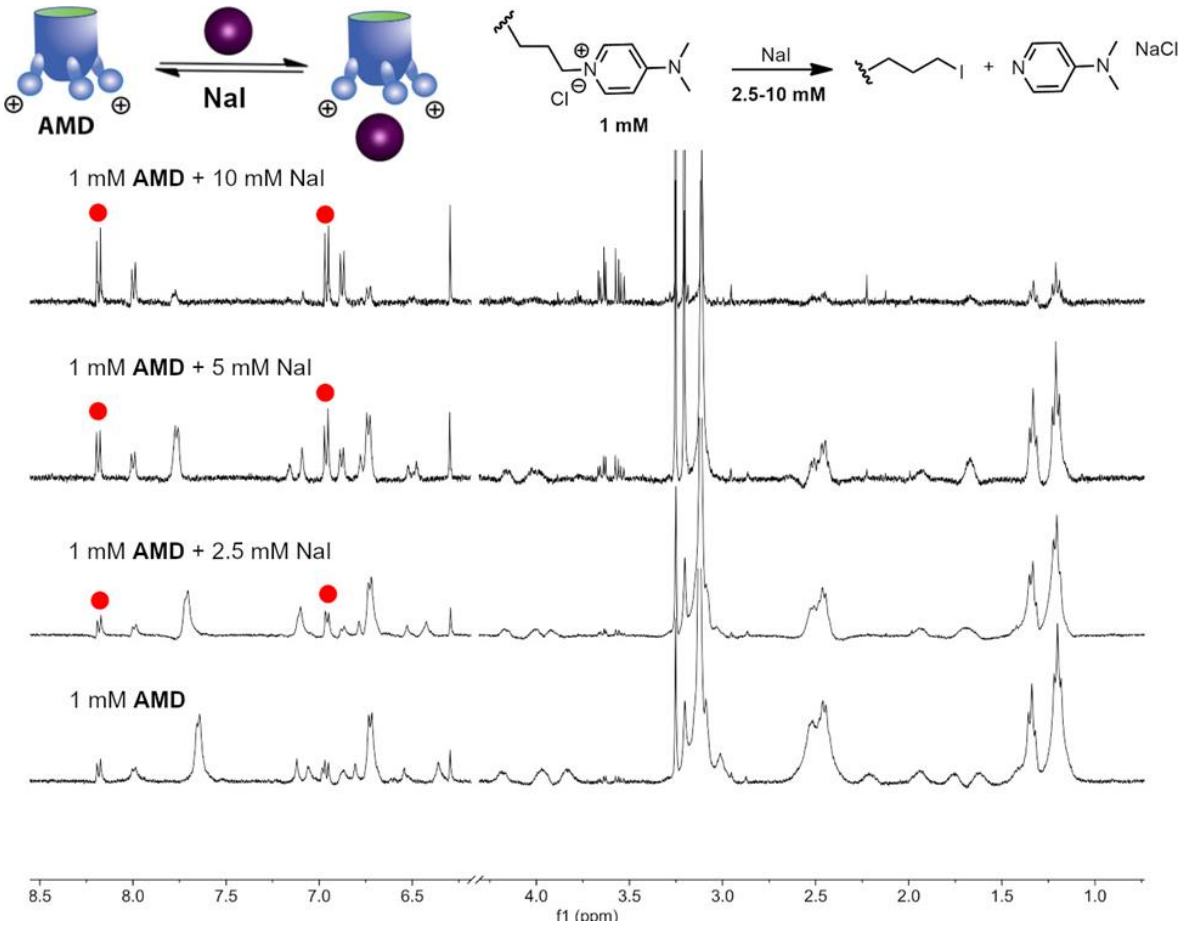

Figure 6. ^{1}H NMR spectra (600 MHz, D_2O, 298K) of **AMD**:NaI binding. Labeled peaks demonstrated the emergence of free DMAP when the insoluble AM-Iodide cavitand was formed.

CONCLUSION

A key strength of the host:guest sensor array approach is its versatility and adaptability. The modular design of these sensors enables the tailoring of the sensor array to specific target molecules by simply swapping out different fluorescent dyes or cavitands. This customization is particularly important given the complexity and diversity of biomolecules, which often require a targeted and specialized approach for analysis.

To further enhance the understanding of host:guest interactions, titration experiments using ^{1}H NMR were conducted to gain insights into the mechanism and orientation of the fluorescent dye within the host cavity. The binding competition between the target molecule and dyes of varying affinities is crucial for differential sensing. Additionally, the presence of anions at the cavitand base can alter the dye response, leading to changes in proton signals and the emergence of peaks in spectra. This synergistic interaction is likely due to displacement of the dye by the anions or bending of the cavitand walls caused by charge effects.

The use of multiple dyes and hosts in the sensor array produces complex signals that can be analyzed using pattern recognition algorithms. This approach offers more diverse signals than using a single fluorescent probe, enabling the sensing array to identify and differentiate small variations in target structure. Host:guest sensor arrays have several advantages over traditional spectroscopic methods, including the ability to monitor biomolecular reactions in real-time, facilitating dynamic monitoring of biological processes. Additionally, their high-throughput screening capability makes them well-suited for drug discovery and other applications requiring high throughput analysis. By combining the power of pattern recognition-based sensing with the versatility of supramolecular chemistry, host:guest sensor arrays represent a promising approach for the analysis of biomolecules in complex biological systems.

EXPERIMENTAL SECTION

I. General Information

^{1}H spectra were recorded on a Bruker Avance NEO 400 MHz or Bruker Avance NEO 600 MHz NMR spectrometer. The spectrometers were automatically tuned and matched to the correct nuclei frequencies. Proton (^{1}H) chemical shifts are reported in parts per million (δ) with respect to tetramethylsilane (TMS, δ=0), and referenced internally. All NMR spectra were processed using MestReNova by Mestrelab. Deuterated NMR solvents were obtained from Cambridge Isotope Laboratories, Inc., Andover, MA, and used without further purification. Solvents were dried through a commercial solvent purification system (Pure Process Technologies, Inc.). Oligonucleotides were purchased from Integrated DNA Technologies (IDT) with standard desalting and no further purification. All other materials were obtained from Aldrich Chemical Company (St. Louis, MO), or Fisher Scientific (Fairlawn, NJ), and were used as received. Fluorescence measurements were performed with a BioTek Synergy H1 Hybrid Multi-Mode Microplate Reader at Fluorescence Endpoint or Spectral scanning read mode with the Ex/Em wavelengths at 480/600 nm (**4-DSMI**), 500/600 nm (**PSMI**), 480/580 nm (**2-DSMI**), 540/600 nm (**DTMI**), 440/580 nm (**2-SMIQ**), with default Gain value=100 unless specifically emphasized. UV-Vis absorbance measurements were performed with an Agilent Technologies Cary 60 UV/Vis spectrophotometer using Brandtech ultra-micro cuvettes (path length=10 mm). A series of titration experiments were conducted to investigate the mode of sensing, and interaction mechanism of cavitands with dyes and anions. The binding of dyes to cavitands can alter the photophysical properties and effective charge of the cavitand, as well as its reactivity towards analytes. Depending on the combination of cavitand and dye, selectivity can be observed either at the pocket or the base of the cavitand. Moreover, a sort of dual-mode binding was discovered and

characterized, wherein the host can bind to both the dye and analyte simultaneously.[9,10] The formation of cavitand:dye complexes, and the changes induced by increasing host concentrations, were assessed by ^{1}H NMR spectroscopy.

II. Cavitand:Dye General Titration Experiments

To prepare the sample, 1 equivalent of cavitand was dissolved in 0.5 mL of deuterated oxide (D_2O) within an NMR tube. Next, 0.5 equivalents of dye were added, and the mixture was subjected to a brief period of ultra-sonication to aid in dissolution. This process was repeated for subsequent additions of 1 and 2 equivalents of dye. It is important to note that some combinations of cavitand and dye were not observable or recordable, likely due to the insolubility of certain cavitands in the presence of D_2O solvent, or the potential formation of aggregates within the solution. As the concentration of the host increased, insolubility within the solution became more prominent, indicating the possibility of such an outcome.

III. Cavitand:Anion General Titration Experiments

To prepare the sample, 1 equivalent of cavitand was dissolved in 0.3 mL of D_2O within an NMR tube. Next, 1 equivalent of a halide salt (NaCl, NaBr, and NaI) was added, and the mixture was subjected to a brief period of ultra-sonication to aid in dissolution. This process was repeated for subsequent additions of 2, 2.5, and 5 equivalents of each salt. It is important to note that certain combinations of cavitand and anion were not able to be observed or recorded, for reasons similar to those previously outlined.

IV. Synthesis of Novel Dyes

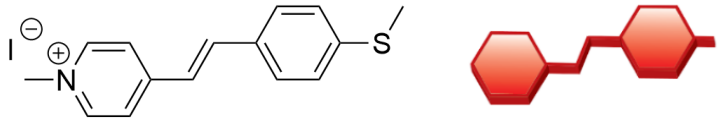

(E)-1-methyl-4-(4-(methylthio)styryl)pyridin-1-ium iodide (SMITE):

1,4-dimethylpyridinium iodide (235 mg, 1.0 mmol) and 4-(methylthio)benzaldehyde (152 mg, 1.0 mmol) were dissolved in ethanol (5 mL) in a round bottom flask. While stirring, one drop of piperidine was added and the resulting solution was refluxed for 12 hr. The reaction was cooled, then diluted with water (10 mL). The resulting precipitate was filtered, rinsed with water and cold ethanol, then dried under vacuum to yield (E)-1-methyl-4-(4-(methylthio)styryl)pyridin-1-ium iodide (340 mg, 92% yield) as a dark yellow powder. ^{1}H NMR (400 MHz, DMSO-d_6) δ 8.83 (d, J = 6.8 Hz, 1H), 8.18 (d, J = 6.9 Hz, 1H), 7.97 (d, J = 16.4 Hz, 1H), 7.69 (d, J = 8.5 Hz, 1H), 7.47 (d, J = 16.4 Hz, 1H), 7.36 (d, J = 8.5 Hz, 1H), 4.24 (s, 3H), 2.53 (s, 3H). Spectrum in **Figure A1**.

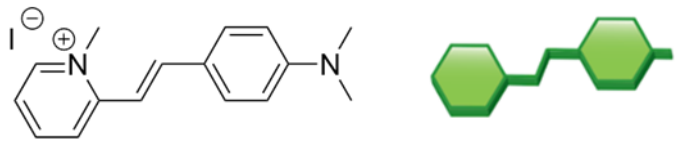

(E)-2-(4-(dimethylamino)styryl)-1-methylpyridin-1-ium iodide (2-DSMI):

1,2-dimethylpyridinium iodide (235 mg, 1.00 mmol) and 4-dimethylaminobenzaldehyde (149 mg, 1.00 mmol) were dissolved in ethanol (5 mL) inside a round bottom flask. While stirring, one drop of piperidine was added and the resulting solution was refluxed for 12 hours. The reaction was cooled, then diluted with water (10 mL). The resulting precipitate was filtered, rinsed with water and cold ethanol, then dried under vacuum to yield (E)-2-(4-(dimethylamino)styryl)-1-methylpyridin-1-ium iodide (343 mg, 94% yield) as a bright red powder. ^{1}H NMR (400 MHz,

DMSO-d_6) δ 8.75 (dd, J = 6.4, 1.5 Hz, 1H), 8.44 (dd, J = 8.6, 1.5 Hz, 1H), 8.34 (td, J = 8.4, 1.4 Hz, 1H), 7.92 (d, J = 15.7 Hz, 1H), 7.70 (m, 3H), 7.24 (d, J = 15.7 Hz, 1H), 6.79 (d, J = 8.9 Hz, 2H), 4.29 (s, 3H), 3.04 (s, 6H). Spectrum in **Figure A2**.

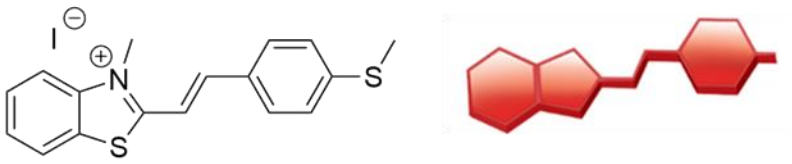

(E)-3-methyl-2-(4-(methylthio)styryl)benzothiazol-3-ium (SMITH):

2-methylbenzothiazole (200µL, 1.60 mmol) was dissolved in ethanol (5 mL), iodomethane (1 mL) was added to the reaction mixture while stirring and the reaction was refluxed for 12 hours. The solution was diluted with diethyl ether (10 mL) and the resulting precipitate was filtered, then rinsed with diethyl ether and dried under vacuum to yield 2,3-dimethylbenzothiazol-3-ium iodide (398 mg, 87%) as a white solid. 1H NMR (400 MHz, DMSO-d_6) δ 8.43 (dd, J = 8.0, 1.3 Hz, 1H), 8.29 (dt, J = 8.5, 1.2 Hz, 1H), 7.90 (dt, J = 8.5, 1.3 Hz, 1H), 7.81 (dd, J = 8.0, 1.2 Hz, 1H), 4.20 (s, 3H), 3.17 (s, 3H). 2,3-dimethylbenzothiazol-3-ium iodide (290mg, 1.00 mmol) and 4-(methylthio)benzaldehyde (152 mg, 1.00 mmol) were dissolved in ethanol (5 mL) inside a round bottom flask. While stirring, one drop of piperidine was added and the resulting solution was refluxed for 12 hours. The reaction was cooled, then diluted with water (10 mL). The resulting precipitate was filtered, rinsed with water and cold ethanol, then dried under vacuum to yield (E)-3-methyl-2-(4-(methylthio)styryl)benzothiazol-3-ium (395 mg, 93% yield) as a dark red powder. ^{1}H NMR (400 MHz, DMSO-d_6) δ 8.42 (dd, J = 7.9, 1.5 Hz, 1H), 8.27 (dd, J = 7.7, 1.1, 1H), 8.06 (d, J = 15.3, 1H), 7.78 (d, J = 8.8 Hz, 2H), 7.56 (td, J = 7.9, 1.1 Hz, 1H), 7.45 (td, J = 7.7, 1.5 Hz, 1H), 7.74 (d, S-15 J = 15.3 Hz, 1H), 6.96 (d, J = 8.8 Hz, 2H), 4.33 (s, 3H), 2.58 (s, 3H). Spectrum in **Figure A3**.

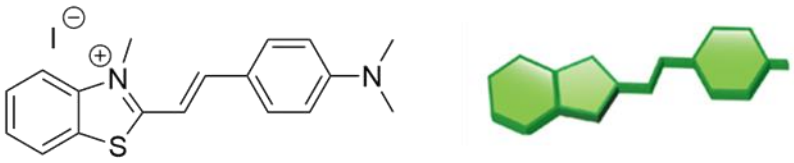

(E)-2-(4-(dimethylamino)styryl)-3-methylbenzothiazol-3-ium iodide (DTMI):

2-methylbenzothiazole (200µL, 1.60 mmol) was dissolved in ethanol (5 mL), iodomethane (1 mL) was added to the reaction mixture while stirring and the reaction was refluxed for 12 hours. The solution was diluted with diethyl ether (10 mL) and the resulting precipitate was filtered, then rinsed with diethyl ether and dried under vacuum to yield 2,3-dimethylbenzothiazol-3-ium iodide (398 mg, 87%) as a white solid. 1H NMR (400 MHz, DMSO-d_6) δ 8.43 (dd, J = 8.0, 1.3 Hz, 1H), 8.29 (dt, J = 8.5, 1.2 Hz, 1H), 7.90 (dt, J = 8.5, 1.3 Hz, 1H), 7.81 (dd, J = 8.0, 1.2 Hz, 1H), 4.20 (s, 3H), 3.17 (s, 3H). 2,3-dimethylbenzothiazol-3-ium iodide (290 mg, 1.00 mmol) and 4-(dimethylamino)benzaldehyde (149 mg, 1.00 mmol) were dissolved in ethanol (5 mL) inside a round bottom flask. While stirring, one drop of piperidine was added and the resulting solution was refluxed for 12 hours. The reaction was cooled, then diluted with water (10 mL). The resulting precipitate was filtered, rinsed with water and cold ethanol, then dried under vacuum to yield (E)-2-(4-(dimethylamino)styryl)-3-methylbenzothiazol-3-ium iodide (386 mg, 92% yield) as a dark purple powder. ^{1}H NMR (400 MHz, DMSO-d_6) δ 8.32 (dd, J = 7.9, 1.5 Hz, 1H), 8.11 (dd, J = 7.7, 1.1, 1H), 8.09 (d, J = 15.3, 1H), 7.93 (d, J = 8.8 Hz, 2H), 7.80 (td, J = 7.9, 1.1 Hz, 1H), 7.70 (td, J = 7.7, 1.5 Hz, 1H), 7.65 (d, S-15 J = 15.3 Hz, 1H), 6.87 (d, J = 8.8 Hz, 2H), 4.24 (s, 3H), 3.13 (s, 6H). Spectrum in **Figure A4**.

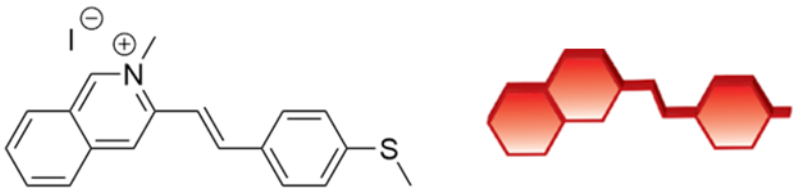

(E)-1-methyl-2-(4-(methylthio)styryl)quinolin-1-ium iodide (2-SMIQ):

2-methylquinoline (250 µL, 1.88 mmol) was dissolved in ethanol (3 mL), iodomethane (0.5 mL) was added to the reaction mixture while stirring and the reaction was refluxed for 12 hours. The solution was diluted with diethyl ether (10 mL) and the resulting precipitate was filtered, then rinsed with diethyl ether and dried under vacuum to yield 1,2-dimethylquinolin-1-ium iodide (457 mg, 85%) as a yellow powder. 1H NMR (400 MHz, DMSO-d_6) δ 9.09 (d, J = 8.5 Hz, 1H), 8.59 (d, J = 9.1 Hz, 1H), 8.40 (d, J = 8.0 Hz, 1H), 8.23 (t, J = 8.0 Hz, 1H), 8.12 (d, J = 8.6 Hz, 1H), 7.99 (t, J = 7.5 Hz, 1H), 4.44 (s, 3H), 3.07 (s, 3H). 1,2-dimethylquinolin-1-ium iodide (150 mg, 0.50 mmol) and 4-(methylthio)benzaldehyde (70 µL, 0.50 mmol) were dissolved in ethanol (5 mL) inside a round bottom flask. While stirring, one drop of piperidine was added and the resulting solution was refluxed for 12 hours. The reaction was cooled, then diluted with water (10 mL). The resulting precipitate was filtered, rinsed with water and cold ethanol, then dried under vacuum then recrystallized with toluene to yield (E)-1-methyl2-(4-(methylthio)styryl)quinolin-1-ium iodide (134 mg, 61% yield) as a dark purple powder. ^{1}H NMR (400 MHz, DMSO-d_6) δ 9.05 (d, J = 8.9 Hz, 1H), 8.57 (dd, J = 9.0, 6.1 Hz, 2H), 8.35 (dd, J = 8.1, 1.6 Hz, 1H), 8.25 – 8.14 (m, 2H), 8.00 – 7.92 (m, 3H), 7.90 (d, J = 11.9 Hz, 1H), 7.42 (d, J = 8.5 Hz, 2H), 4.56 (s, 3H), 2.57 (s, 3H). Spectrum in **Figure A5**.

APPENDIX

NMR Spectral Data of Components Used

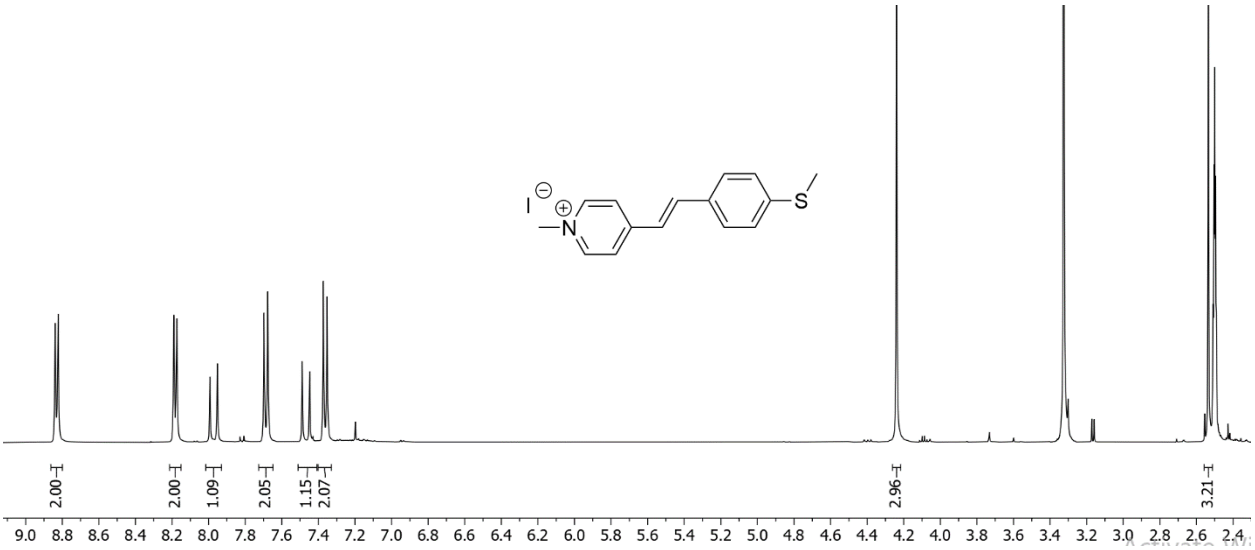

Figure A1. ^{1}H NMR spectrum of **SMITE** (400 MHz, DMSO-d_6, 298K).

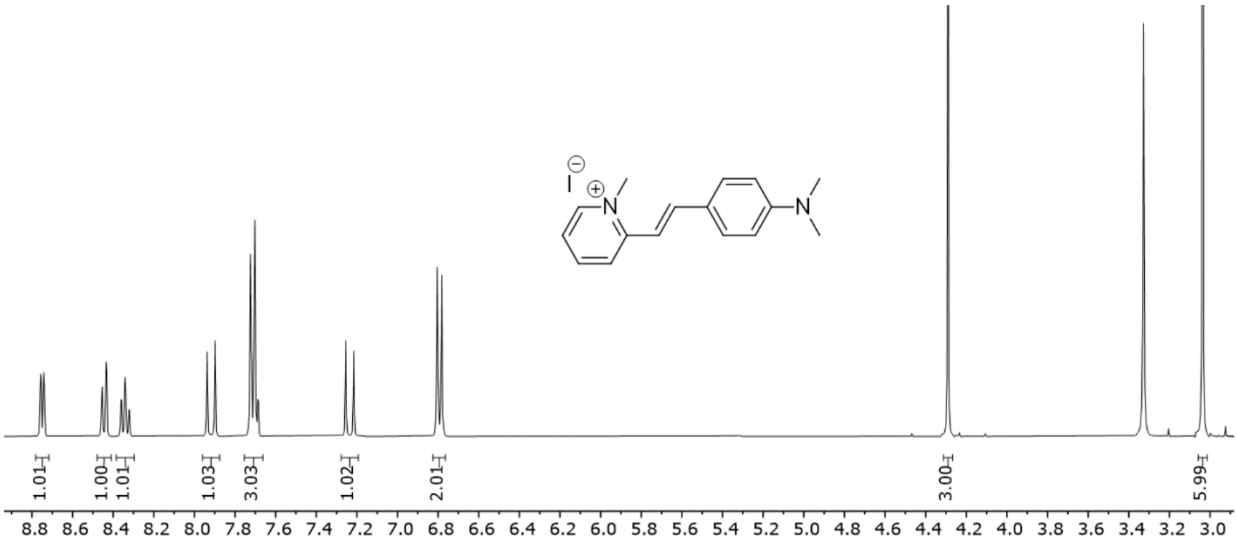

Figure A2. ^{1}H NMR spectrum of **2-DSMI** (400 MHz, DMSO-d_6, 298K).

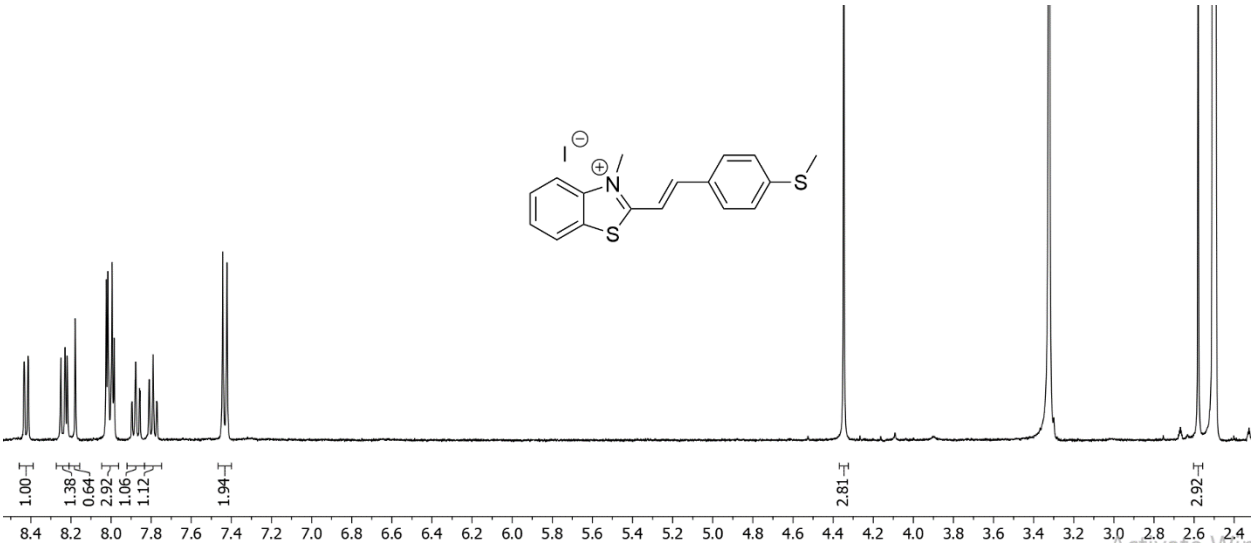

Figure A3. ^{1}H NMR spectrum of **SMITH** (400 MHz, DMSO-d_6, 298K).

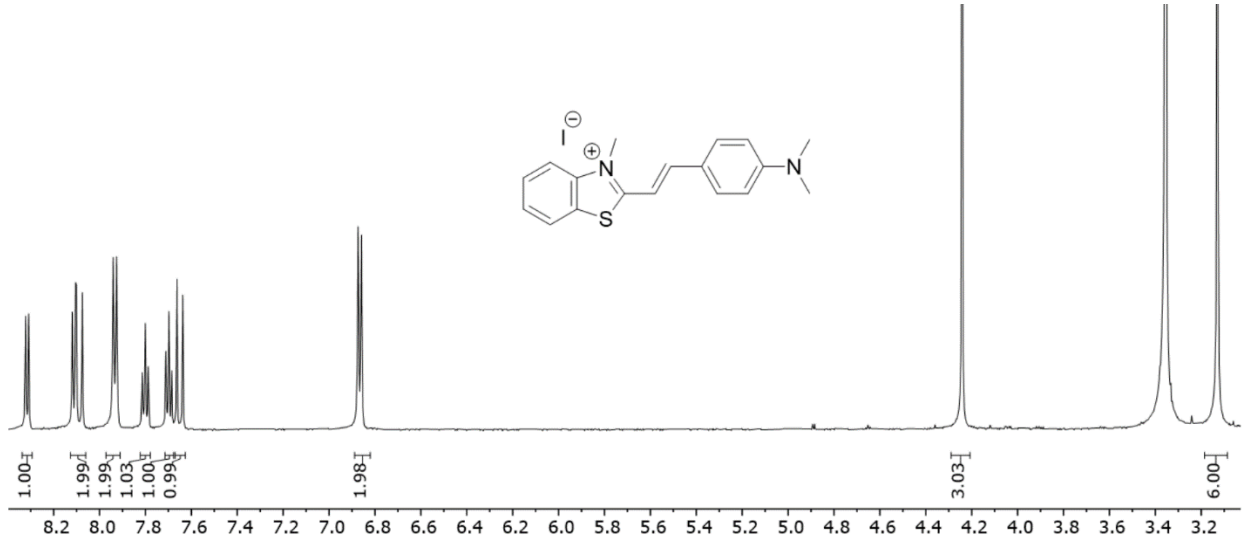

Figure A4. ^{1}H NMR spectrum of **DTMI** (400 MHz, DMSO-d_6, 298K).

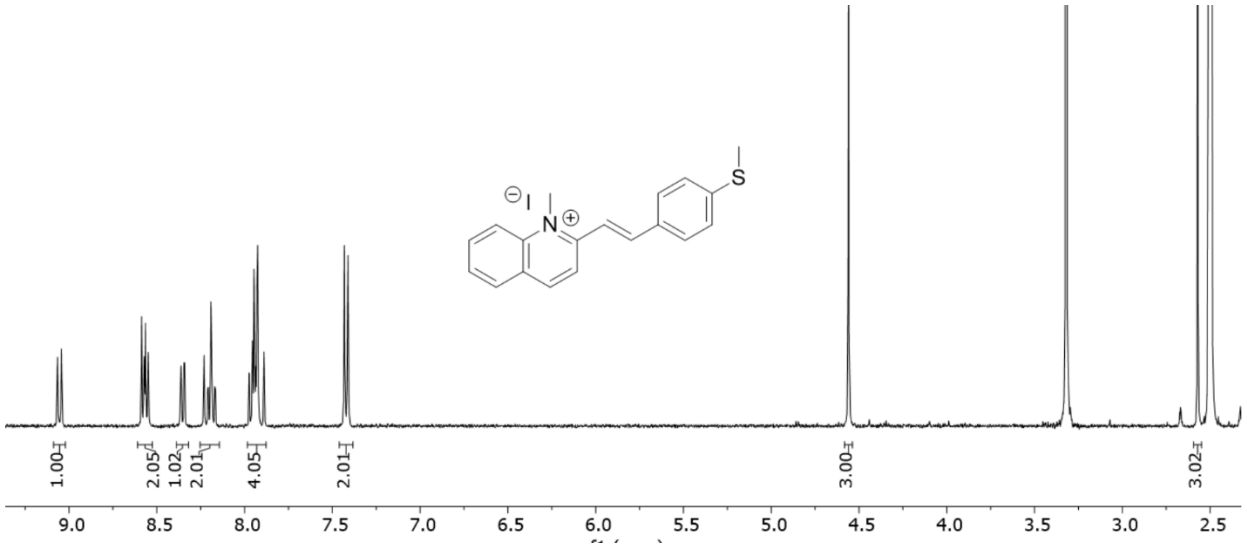

Figure A5. ^{1}H NMR spectrum of **2-SMIQ** (400 MHz, DMSO-d_6, 298K).

REFERENCES

Aziz, Hannah R., et al. “Dual Binding Modes of a Small Cavitand.” *Supramolecular Chemistry*, Taylor and Francis, Oct. 2021, pp. 1–6. https://doi.org/10.1080/10610278.2021.1987433.

Chen, Junyi, Adam D. Gill, et al. “Machine Learning Aids Classification and Discrimination of Noncanonical DNA Folding Motifs by an Arrayed Host:Guest Sensing System.” *Journal of the American Chemical Society*, vol. 143, no. 32, American Chemical Society, Aug. 2021, pp. 12791–99. https://doi.org/10.1021/jacs.1c06031.

Chen, Junyi, Briana L. Hickey, Lin-Lin Wang, et al. “Selective Discrimination and Classification of G-quadruplex Structures With a Host–guest Sensing Array.” *Nature Chemistry*, vol. 13, no. 5, Nature Portfolio, Apr. 2021, pp. 488–95. https://doi.org/10.1038/s41557-021-00647-9.

Chen, Junyi, Briana L. Hickey, Ziting Gao, et al. “Sensing Base Modifications in Non-Canonically Folded DNA With an Optimized Host:Guest Sensing Array.” *ACS Sensors*, vol. 7, no. 8, American Chemical Society, Aug. 2022, pp. 2164–69. https://doi.org/10.1021/acssensors.2c00839.

Gill, Adam D., Briana L. Hickey, Wenwan Zhong, et al. “Selective Sensing of THC and Related Metabolites in Biofluids by Host:Guest Arrays.” *Chemical Communications*, vol. 56, no. 31, Royal Society of Chemistry, Apr. 2020, pp. 4352–55. https://doi.org/10.1039/d0cc01489c.

Gill, Adam D., Briana L. Hickey, Siwen Wang, et al. “Sensing of Citrulline Modifications in Histone Peptides by Deep Cavitand Hosts.” *Chemical Communications*, vol. 55, no. 88, Royal Society of Chemistry, Oct. 2019, pp. 13259–62. https://doi.org/10.1039/c9cc07002h.

Hickey, Briana L., Junyi Chen, et al. “Enantioselective Sensing of Insect Pheromones in Water.” *Chemical Communications*, vol. 57, no. 98, Royal Society of Chemistry, Dec. 2021, pp. 13341–44. https://doi.org/10.1039/d1cc05540b.

Hickey, Briana L., Alexie Andrea P. Raz, et al. “Selective Anion Recognition and Sensing in High Salt Water With Cationic Deep Cavitands.” *Chemical Communications*, forthcoming.

Liu, Yang, Lizeth Perez, Magi Mettry, Connor J. Easley, et al. “Self-Aggregating Deep Cavitand Acts as a Fluorescence Displacement Sensor for Lysine Methylation.” *Journal of the American Chemical Society*, vol. 138, no. 34, American Chemical Society, Aug. 2016, pp. 10746–49. https://doi.org/10.1021/jacs.6b05897.

Liu, Yang, Lizeth Perez, Magi Mettry, Adam D. Gill, et al. “Site Selective Reading of Epigenetic Markers by a Dual-mode Synthetic Receptor Array.” *Chemical Science*, vol. 8, no. 5, Royal Society of Chemistry, May 2017, pp. 3960–70. https://doi.org/10.1039/c7sc00865a.

Zhong, Wenwan, and Richard J. Hooley. “Combining Excellent Selectivity With Broad Target Scope: Biosensing With Arrayed Deep Cavitand Hosts.” *Accounts of Chemical Research*, vol. 55, no. 7, American Chemical Society, Mar. 2022, pp. 1035–46. https://doi.org/10.1021/acs.accounts.2c00026.